

Electrochemical H₂O₂ - stat mode as reaction concept to improve the process performance of an unspecific peroxygenase

Giovanni V. Sayoga^{a,*}, Victoria S. Bueschler^a, Hubert Beisch^b, Tyll Utesch^c, Dirk Holtmann^d, Bodo Fiedler^b, Daniel Ohde^a, Andreas Liese^{a,*}

^a Institute of Technical Biocatalysis, Hamburg University of Technology, Denickestraße 15, 21073 Hamburg, Germany

^b Institute of Polymers and Composites, Hamburg University of Technology, Denickestraße 15, 21073 Hamburg, Germany

^c Institute of Bioprocess and Biosystems Engineering, Hamburg University of Technology, Denickestraße 15, 21073 Hamburg, Germany

^d Institute of Process Engineering in Life Sciences, Karlsruhe Institute of Technology, Fritz-Haber-Weg 4, 76131 Karlsruhe, Germany

ARTICLE INFO

Keywords:

Biocatalysis
Bioelectrochemical system
Bioelectrocatalysis
Electrosynthesis
Hydrogen peroxide

ABSTRACT

The electroenzymatic hydroxylation of 4-ethylbenzoic acid catalyzed by the recombinant unspecific peroxygenase from the fungus *Agrocybe aegerita* (rAaeUPO) was performed in a gas diffusion electrode (GDE)-based system. Enzyme stability and productivity are significantly affected by the way the co-substrate hydrogen peroxide (H₂O₂) is supplied. In this study, two *in-situ* electrogeneration modes of H₂O₂ were established and compared. Experiments under galvanostatic conditions (constant productivity of H₂O₂) were conducted at current densities spanning from 0.8 mA cm⁻² to 6.4 mA cm⁻². For comparison, experiments under H₂O₂-stat mode (constant H₂O₂ concentration) were performed. Here, four H₂O₂ concentrations between 0.06 mM and 0.28 mM were tested. A maximum H₂O₂ productivity of 5.5 μM min⁻¹ cm⁻² and productivity of 10.5 g L⁻¹ d⁻¹ were achieved under the galvanostatic condition at 6.4 mA cm⁻². Meanwhile, the highest total turnover number (TTN) of 710,000 mol mol⁻¹ and turnover frequency (TOF) of 87.5 s⁻¹ were obtained under the H₂O₂-stat mode at concentration limits of 0.15 mM and 0.28 mM, respectively. The most favorable outcome in terms of maximum achievable TTN, TOF and productivity was found under the H₂O₂-stat mode at concentration limit of 0.2 mM. Here, a TTN of 655,000 mol mol⁻¹, a TOF of 80.3 s⁻¹ and a productivity of 6.1 g L⁻¹ d⁻¹ were achieved. The electrochemical H₂O₂-stat mode not only offers a promising alternative reaction concept to the well-established galvanostatic mode but also enhances the process performance of unspecific peroxygenases.

Introduction

The unspecific peroxygenase (UPO) from the basidiomycete fungus *Agrocybe aegerita* (AaeUPO) (EC 1.11.2.1) was first discovered and documented in 2004 [1]. Since then, UPO has attracted a lot of interest due to its ability to selectively introduce oxygen atoms into various organic molecules such as benzene, pyridine and cyclohexane and derivatives thereof [2]. UPO catalyzes, among others, epoxidation of alkenes, hydroxylation of alkanes, oxidation of aromatics and *N*-dealkylations [3]. This feature has also drawn the attention of organic chemists, since oxyfunctionalization is one of the most challenging

chemical reactions in organic synthesis, especially, the oxyfunctionalization of unactivated C-H bonds [2,4]. Until recently, research on cytochrome P450 monooxygenases was mainly in focus for the enzymatic selective introduction of oxygen functionalities [5,6]. While P450 monooxygenases are able to incorporate oxygen into organic substrates, these enzymes are relatively unstable, dependent on an expensive cofactor and have low catalytic activity [5–7]. In comparison, UPOs are fairly stable and require only hydrogen peroxide (H₂O₂), acting simultaneously as the oxygen donor and the electron acceptor [5].

Despite their relative high stability, UPOs still suffer from

Abbreviations: AaeUPO, unspecific peroxygenase from *Agrocybe aegerita*; ABTS, 2,2'-azino-bis(3-ethylbenzothiazoline-6-sulfonic acid); CPO, chloroperoxidase; EBA, 4-ethylbenzoic acid; F.E., Faradaic efficiency; GDE, gas diffusion electrode; GOx, glucose oxidase; HEBA, 4-(1-hydroxyethyl)benzoic acid; KP_i, potassium phosphate buffer; rAaeUPO, recombinant unspecific peroxygenase from *Agrocybe aegerita*; TOF, turnover frequency; TON, turnover number; TTN, total turnover number; UPO, unspecific peroxygenase.

* Corresponding authors.

E-mail addresses: giovanni.sayoga@tuhh.de (G.V. Sayoga), liese@tuhh.de (A. Liese).

<https://doi.org/10.1016/j.nbt.2023.10.007>

Received 16 September 2023; Received in revised form 10 October 2023; Accepted 15 October 2023

Available online 16 October 2023

1871-6784/© 2023 The Authors. Published by Elsevier B.V. This is an open access article under the CC BY license (<http://creativecommons.org/licenses/by/4.0/>).

inactivation at an elevated concentration of its co-substrate H_2O_2 [8]. This is one reason why the full technical application of UPOs is still limited [8]. There are several established methods already reported to mitigate the inactivating effect of H_2O_2 . The approaches mainly focus on the adjustment of reaction conditions, especially to keep a constantly low H_2O_2 concentration. Feeding a diluted H_2O_2 solution into a reaction medium has been shown to be able to increase the total turnover number (TTN) [9], which is defined as the quotient of moles of the product generated after the enzyme was deactivated and the moles of the used enzyme. However, this approach leads to a volume increase and high local H_2O_2 concentrations [10]. As a result, several *in-situ* H_2O_2 generation methods have been investigated. *In-situ* generation of H_2O_2 can be accomplished through various approaches, including the utilization of a chemical reductant such as dihydroxyfumaric acid [11], an enzyme e.g., glucose oxidase (GOx) [12], a piezocatalytic method [13], photocatalysis [14] or an electrochemical method [15].

Lately, the application of a specific electrode type called gas diffusion electrode (GDE) has been expanded, particularly in the electrochemical reduction of O_2 to H_2O_2 [16]. The GDE possesses a three-phase boundary consisting of a gas, liquid and solid phase [16]. This enables a direct and higher mass transport of O_2 from the atmosphere through the electrode and in contact with the electrolyte [16]. Thus, limitations due to low O_2 solubility and diffusivity in the liquid and towards the electrode are avoided [17]. The combination of the *in-situ* generation of H_2O_2 and the subsequent biocatalytic reaction has been reported. Examples are the oxidation of thioanisole catalyzed by the chloroperoxidase (CPO) from *Caldariomyces fumago* [10,15], the halogenation of 4-pentenoic acid catalyzed by the vanadium CPO from *Curvularia inaequalis* [18], and the hydroxylation of ethylbenzene catalyzed by the recombinant *AaeUPO* (*rAaeUPO*) [19]. The electrochemical *in-situ* H_2O_2 generation method does not increase the reaction volume and avoids the formation of by-products (e.g., gluconic acid), which may occur when using diluted H_2O_2 solution or enzymatic *in-situ* H_2O_2 generation with GOx, respectively [10].

Usually, H_2O_2 is generated *in-situ* at a constant rate (galvanostatic) [10,15,18–20]. However, this approach leads to an accumulation of H_2O_2 in the medium as the enzyme activity constantly decreases due to H_2O_2 -dependent enzyme deactivation, the so-called catalase malfunction reaction [8]. In turn, accumulation of H_2O_2 further increases the enzyme deactivation rate. It has been demonstrated that by keeping the H_2O_2 concentration constant (H_2O_2 -stat mode), by adjusting the feeding rate of H_2O_2 to a set H_2O_2 concentration of 50 μM , the enzyme operational stability could be increased, compared to the continuous addition of H_2O_2 [9]. Moreover, the H_2O_2 -stat mode was implemented within the bioelectrochemical system, with H_2O_2 concentration limits set at 0.5 mM and 1.2 mM [21]. Nevertheless, due to relative high H_2O_2 concentration thresholds the enzyme operational stability and the final obtained product concentration were low compared to the galvanostatic mode [21].

In this study, the hydroxylation of 4-ethylbenzoic acid (EBA) catalyzed by *rAaeUPO* was performed in a GDE system. Two electro-generation modes were employed to supply the H_2O_2 *in-situ*. 1) A H_2O_2 -stat mode at a concentration limit set between 0.06 mM and 0.28 mM. A custom automation program was developed to regulate the current output of the power supply to the GDE. This program utilized the input from the H_2O_2 sensor to ensure a constant H_2O_2 concentration (Fig. 1). 2) A galvanostatic mode at a constant current density between 0.8 mA cm^{-2} and 6.4 mA cm^{-2} , which served as an internal benchmark. The TTN, turnover frequency (TOF) and the productivity were determined and compared. The objective is to find the optimal H_2O_2 concentration limit under the H_2O_2 -stat mode, which would enable a high TOF while maintaining a high TTN.

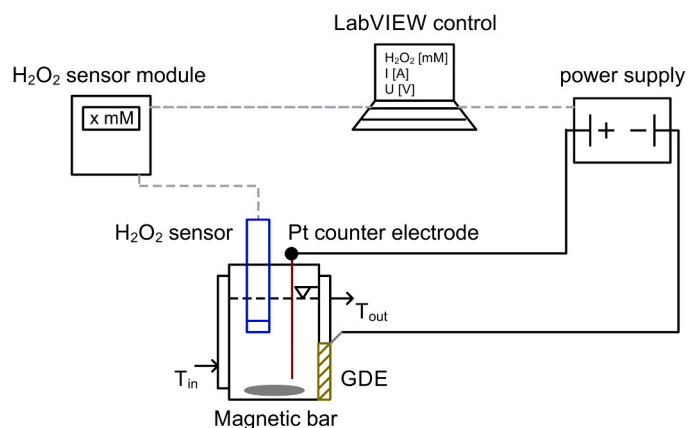


Fig. 1. Schematic representation of the complete electroenzymatic reaction system, including the H_2O_2 sensor, H_2O_2 sensor module, power supply and Lab VIEW control unit. The control unit is used to regulate the current output sent to the electrodes and to maintain a constant H_2O_2 concentration. GDE: gas diffusion electrode (working electrode), Pt: platinum (counter electrode). Dashed line: working cycle of the automation system. Solid line: electric circuit between the power supply and the electrodes.

Material and methods

Materials

Unless otherwise stated, all chemicals were purchased from Carl Roth (Karlsruhe, Germany) or Sigma Aldrich (Steinheim, Germany) in a purity $\geq 98\%$. HEBA ($\geq 97\%$) was purchased from BLD Pharm (China). 2,2'-azino-bis(3-ethylbenzothiazoline-6-sulfonic acid) (ABTS) ($\geq 98\%$) was purchased from TCI (Eschborn, Germany).

Production of his-tagged *rAaeUPO*

The inoculum seed of *Pichia pastoris* (X33), which expresses the recombinant protein *rAaeUPO*-PaDa-I-C6His was prepared as described in [22], in a 50 mL buffered complex glycerol medium (BMGY) containing 25 $\mu\text{g mL}^{-1}$ Zeocin. The main fermentation was conducted in a 1 L DASGIP bioreactor system (Eppendorf, Hamburg, Germany) and performed as stated in [22]. Modifications to the fermentation process are described in the following. The glycerol batch phase was started by cultivating the inoculum in a 500 mL basal salt medium containing 40 g L^{-1} glycerol. Once the initial glycerol was consumed as indicated by the spike of the dissolved oxygen (DO) signal, the glycerol fed-batch phase was started and maintained for 24 h. Afterwards, the glycerol feed was stopped and the methanol fed-batch phase was started to induce the overexpression of *rAaeUPO*. The DO content and temperature were set at 30% and 30 °C, respectively. To maintain these values, the stirring rate (400–1200 rpm) and aeration rate (30–60 $\text{L h}^{-1} \hat{=} ca. 1 \text{ vvm}$) were regulated automatically by the system. A 25% v/v ammonia solution was used to maintain the pH at 5. The feeding profiles of glycerol and methanol in the fed-batch phase were set as stated in [23]. The biomass was separated from the fermentation broth *via* centrifugation (Beckmann J2HS, Beckmann Coulter, California, USA) at 5000 rpm for 2 h at 4 °C. The supernatant was sterile-filtered (0.22 μm , DURAPORE, Merck Millipore, Massachusetts, USA) and concentrated by ultrafiltration (10 kDa molecular weight cut off, Minimate TFF Capsule, Pall, New York, USA). *rAaeUPO*s were dialyzed and concentrated in 0.1 M potassium phosphate (KP_i) buffer, pH 7.

Determination of enzyme activity and concentration

The enzyme activity was quantified using an ABTS assay. The activity assay was conducted spectrophotometrically (Genesys 180, Thermo Scientific, Massachusetts, USA) at 420 nm for 1 min as technical duplicates. The assay consisted of 750 μL 0.1 M Na_2HPO_4 / 0.1 M citric acid buffer pH 4.4, 100 μL 3 mM ABTS, 50 μL 40 mM H_2O_2 and 100 μL sample. The sample was added last as it starts the reaction. Directly after adding the sample, the reaction mixture was mixed by pipetting up and down 5 times using the sample pipette tip. The rAaeUPO activity and concentration were calculated as shown below, using equations described previously in [24].

$$v = \frac{\text{slope of the absorbance } [\text{min}^{-1}] \bullet 10}{36 [\text{mM}^{-1} \text{ cm}^{-1}] \bullet 1 \text{cm}} \quad (1)$$

$$c_{rAaeUPO} = v \bullet \frac{(k_m + S)}{k_{cat} \bullet S} = v \bullet df \bullet (k_m + S) \bullet \frac{1}{k_{cat} \bullet S} \quad (2)$$

Where v is the rAaeUPO volumetric activity in U mL^{-1} , S is the substrate ABTS concentration in the assay in mM, $c_{rAaeUPO}$ is the rAaeUPO concentration in μM , k_m is the Michaelis-Menten parameter (50 μM) [5], k_{cat} is the catalytic rate constant (546 s^{-1}) [5] and df is the dilution factor (10, 5 or 1).

Offline H_2O_2 determination

H_2O_2 concentrations were determined photometrically (lower detection limit of 10 μM) [25]. The assay (1 mL) contained the sample, iodide reagent (0.4 M potassium iodide, 0.05 M NaOH, 10^{-4} M ammonium molybdate) and 0.5 M potassium hydrogen phthalate in a ratio of 4:3:3. The treated sample was measured directly at 351 nm in technical duplicates. Calibration curves (10–100 μM) were prepared using diluted H_2O_2 solution.

Determination of 4-ethylbenzoic acid (EBA) and 4-(1-hydroxyethyl)benzoic acid (HEBA)

EBA and HEBA concentrations were quantified using a Nexera LC-40 HPLC system (Shimadzu, Kyoto, Japan) equipped with a UV-Vis SPD-40 detector (Shimadzu, Kyoto, Japan) and an Inertsil ODS-P, C18-RP, 5 μm , 100 \AA column (GL Science, Japan). Sample preparation and chromatography analysis were carried out following the procedures described in [26]. Calibration curves (0.5–10 mM) were prepared using authentic standards (Suppl. Fig. S1, Fig. S2). All measurements were conducted in technical duplicates.

Electrochemical setup

Electrochemical and electroenzymatic experiments were conducted in an undivided reactor. Carbon black GDE (PerOx with PTFE layer, Gaskatel, Kassel, Germany) (A: 12.56 cm^2 , thickness: 250 μm) served as the working electrode and was fixed at the side of the reactor. One side of the GDE faced the liquid phase, while the other side faced the ambient air. A platinum (Pt) wire (Chempur, Karlsruhe, Germany) (99.9%, A: 1.5 cm^2) served as the counter electrode. Galvanostatic and dynamic electrical currents were generated by a Keithley 2231a-30-3 DC (Tektronix, Oregon, USA) power supply. Stainless steel crocodile clips were used as connectors. The reactor was equipped with a DULCOTEST PEROX H3 E H_2O_2 sensor (ProMinent, Heidelberg, Germany), a DULCOMETER dialog DACb H_2O_2 sensor module (ProMinent, Heidelberg, Germany) and an NI LabVIEW 2021 SP1 virtual instrumentation program (National Instruments, Texas, USA) (Fig. 1). The H_2O_2 sensor has a response time of 45 s with a lower and an upper detection limit of 0.006 mM and 0.294 mM, respectively. A constant H_2O_2 concentration (H_2O_2 -stat mode) in the medium was maintained by employing an

automation program designed in- and controlled by the LabVIEW software (Suppl. Fig. S5). The H_2O_2 concentration was measured by the H_2O_2 sensor and the concentration was transmitted to LabVIEW. LabVIEW controlled the current output of the power supply and based on the set H_2O_2 concentration limit, the electrical current sent to the electrode was adjusted to control the H_2O_2 productivity. For the automation program, the maximum potential, proportional gain and integral time were set to 6 V, 0.01, and 2 min, respectively. The H_2O_2 concentration limit was set either to 0.06 mM, 0.15 mM, 0.2 mM or 0.28 mM. These values were selected to ensure a relatively balanced distribution across the H_2O_2 sensor's limit.

Electroenzymatic experiments

The reaction medium contained 200 mL 0.1 M KPi pH 7, 8 mM EBA and 10 nM of rAaeUPO. The medium was stirred at 250 rpm by a magnetic bar (d: 0.5 cm, l: 3 cm). The experiments were conducted at 22 ± 1 $^\circ\text{C}$ to minimize thermal deactivation of the enzyme. Galvanostatic experiments were performed at electrical current densities between 0.8 mA cm^{-2} and 6.4 mA cm^{-2} . In the H_2O_2 -stat mode, the automation system was engaged. Thus, a dynamic current was applied to the electrodes. Experiments were initiated by either starting the power supply or the automation program. Samples for the quantification of EBA, 4-(1-hydroxyethyl)benzoic acid (HEBA) (20 μL), H_2O_2 concentration (100–800 μL), and rAaeUPO activity (65–200 μL) were taken periodically from the system. Each experiment was stopped when there was no measurable rAaeUPO activity (slope of the absorbance < 0.01 $\text{cm}^{-1} \text{ min}^{-1}$). Unless otherwise stated, electroenzymatic experiments were performed as duplicates. The TOF refers to the turnover number (TON) per unit time (60 min). The TON is described as the quotient of moles of the product generated at a specific time before the enzyme was deactivated and the moles of the used enzyme. The productivity is defined as the mass of product (derived from the final product concentration) per used reactor volume and time.

The H_2O_2 productivity was determined in an abiotic environment (without EBA and rAaeUPO) and in galvanostatic mode (0.8 mA cm^{-2} - 6.4 mA cm^{-2}). The H_2O_2 concentration was measured periodically over the course of 30 min. Duplicates were performed for each current density. The Faradaic efficiency (F.E.) describes how much energy in form of electrons is consumed for the formation of H_2O_2 and the formation of side products. The H_2O_2 F.E. was calculated using the equation given elsewhere [27].

Results and discussion

To determine the optimal H_2O_2 concentration limit for the rAaeUPO-catalyzed hydroxylation of EBA under the H_2O_2 -stat mode in the GDE system, several steps were taken. Initially, the electrochemical characterization of the system was conducted to assess the H_2O_2 productivity. Thereafter, the electroenzymatic hydroxylation of EBA was performed under galvanostatic mode to establish a reference for TOF, TTN, and productivity. Subsequently, electroenzymatic experiments were repeated under H_2O_2 -stat mode. Finally, the TOF, TTN, and productivity obtained from both H_2O_2 electrogeneration methods were compared to identify the most efficient approach and eventually the optimal H_2O_2 concentration limit.

Electroenzymatic hydroxylation of EBA under galvanostatic mode

As a part of the system's electrochemical characterization process in regards to its H_2O_2 generation capabilities, the H_2O_2 productivity was determined at various current densities. The electrochemical characterization was conducted in an abiotic environment, without the enzyme and the substrate.

In Fig. 2A, the accumulated H_2O_2 concentration increased linearly over time for all tested current densities within the 30 min running time.

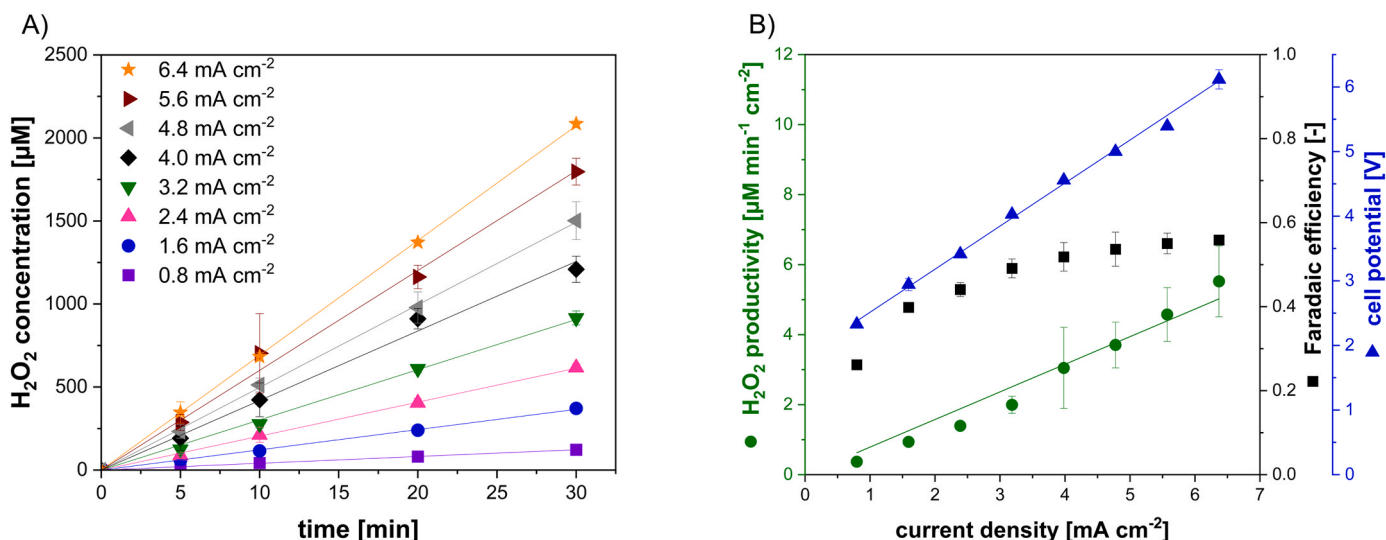


Fig. 2. A) H₂O₂ concentration as a function of time at various current densities. B) H₂O₂ productivity, Faradaic efficiency (F.E.) and resulting cell potential as a function of current density. Reaction conditions: GDE (12.56 cm²), Pt counter electrode (1.5 cm²), 200 mL 0.1 M KP_i pH 7, temperature: 22 ± 1 °C, 250 rpm. F.E. was determined after 30 min. Duplicates were performed. Depicted lines are linear regression fits with R² ≥ 0.99.

Based on these results, it can be concluded that there is no indication of O₂ diffusion and mass transfer limitation at the GDE within the tested range. Additionally, as depicted in the Fig. 2B, H₂O₂ productivities, resulting cell potentials and the F.E.s. are shown as a function of the current density. The H₂O₂ productivity (y [μM min⁻¹ cm⁻²] = 0.79 [μM min⁻¹ mA⁻¹] • J [mA cm⁻²]) and the resulting cell potential (y [V] = 0.67 [V cm² mA⁻¹] • J [mA cm⁻²] + 1.85 [V]) show a linear increase with increasing current density. The maximum H₂O₂ productivity of 5.5 μM min⁻¹ cm⁻² was achieved at 6.4 mA cm⁻², the highest tested current density. The highest H₂O₂ productivity reported here is comparable to those reported in literature for GDE-based systems [18,20,27]. It is also observed in Fig. 2B that the F.E. increases from 0.26 at 0.8 mA cm⁻² to 0.50 at 3.2 mA cm⁻². Upon further increasing the current density, the F.E. shows only minimal improvement and reaches an apparent plateau, with a maximum of 0.55 at 6.4 mA cm⁻². A similar behavior was reported, where the F.E. increased from 0.60 to 0.78 as the current density was increased from 5 mA cm⁻² to 30 mA cm⁻² [19]. A F.E. below 1 means that not all electrons were efficiently used to generate H₂O₂, or the resulting concentration of accumulated H₂O₂ was lower than the theoretical concentration calculated based on the total consumed electrons. Competing reactions such as hydrogen evolution and direct reduction of O₂ to H₂O are known to reduce the F.E. [25,28]. Furthermore, within the electrochemical system the formed H₂O₂ could be further reduced to H₂O, oxidized to radicals or decomposed to O₂ and H₂O, thus reduced the accumulated H₂O₂ concentration [25,26,28]. Surface modification approaches such as thermal oxidation (e.g., using KOH) and coating with carbon nanotubes offer promising ways to enhance the performance of carbon-based electrodes [18,29]. These modifications provide a more active surface with O or OH groups and higher current density, respectively [18,29]. As a result, H₂O₂ generation is effectively promoted, leading to an increase in the F.E. [18,29]. Additionally, minimizing the contact between the formed H₂O₂ and counter electrode by placing the counter electrode in a separate compartment is expected also to increase the F.E. of the system. Overall, obtained F.E.s. in this study are comparable to the reported values in literature for GDE systems and 3D carbon-based electrodes [10,20,27,30,31].

Following the electrochemical characterization, the electroenzymatic hydroxylation of EBA was performed. The electroenzymatic experiments were conducted initially under the galvanostatic mode by applying various current densities between 0.8 mA cm⁻² and 6.4 mA cm⁻². The hydroxylation of EBA was catalyzed by rAaeUPO and

yielded HEBA as the product. Before starting the experiment, rAaeUPO was added to the reaction mixture. A sample was taken to determine the initial activity using the ABTS assay, which was set as 100% relative activity. Throughout the experiment, enzyme activities were measured relative to the initial activity and expressed as the apparent ABTS-activity due to the coexistence of ABTS and EBA in the sample. Fig. 3A-D show the results of electroenzymatic experiments performed at 0.8 mA cm⁻², 2.4 mA cm⁻², 4.0 mA cm⁻² and 5.6 mA cm⁻², respectively. As the current density is increased, the H₂O₂ productivity increases correspondingly from 0.37 to 4.6 μM min⁻¹ cm⁻². In general, it can be observed that for a period of time the reactions reach an apparent equilibrium in terms of the measured H₂O₂ concentration, with higher H₂O₂ concentrations being maintained at increased current densities (Fig. 3E). At the same time, the duration, in which the H₂O₂ concentration remains constant (termed as apparent equilibrium time) shortens (Fig. 3E). This phenomenon occurred because the relative enzyme activity and the catalytic consumption rate of the H₂O₂ decreased over the course of the experiment, while the H₂O₂ productivity remained constant. The apparent equilibrium time was determined using a threshold of 30%, which represents the minimum acceptable deviation from the apparent H₂O₂ equilibrium concentration. This choice was made considering the generally low H₂O₂ concentrations observed during the experiment. Opting for a lower threshold, such as 10%, would have resulted in the inability to differentiate deviations from a lower apparent equilibrium H₂O₂ concentration e.g., 0.13 mM at 2.4 mA cm⁻², or lower. Consequently, deviations below 30% were considered to be minor fluctuations. At low current density, such as 0.8 mA cm⁻², the H₂O₂ generation rate becomes the rate-limiting step of the reaction. As a result, the apparent equilibrium H₂O₂ concentration is among the lowest compared to other current densities, and the apparent equilibrium time is longer (Fig. 3E) due to higher enzyme stability (71 h). However, at current densities ≥ 2.4 mA cm⁻², the catalytic consumption rate of H₂O₂ becomes lower than the H₂O₂ productivity, making the H₂O₂ consumption rate the limiting factor of the reaction and leading to a higher apparent equilibrium H₂O₂ concentration. As more substrate is converted and the enzyme activity gradually decreases, less H₂O₂ is consumed, resulting in its accumulation in the medium. This accumulation triggers a catalase malfunction reaction, causing even faster enzyme deactivation and resulting in a rapid loss of enzyme activity. Consequently, the apparent equilibrium time decreases with increasing current density (Fig. 3E). In the initial phase of the reaction, the product formation exhibits a linearity for all applied current densities.

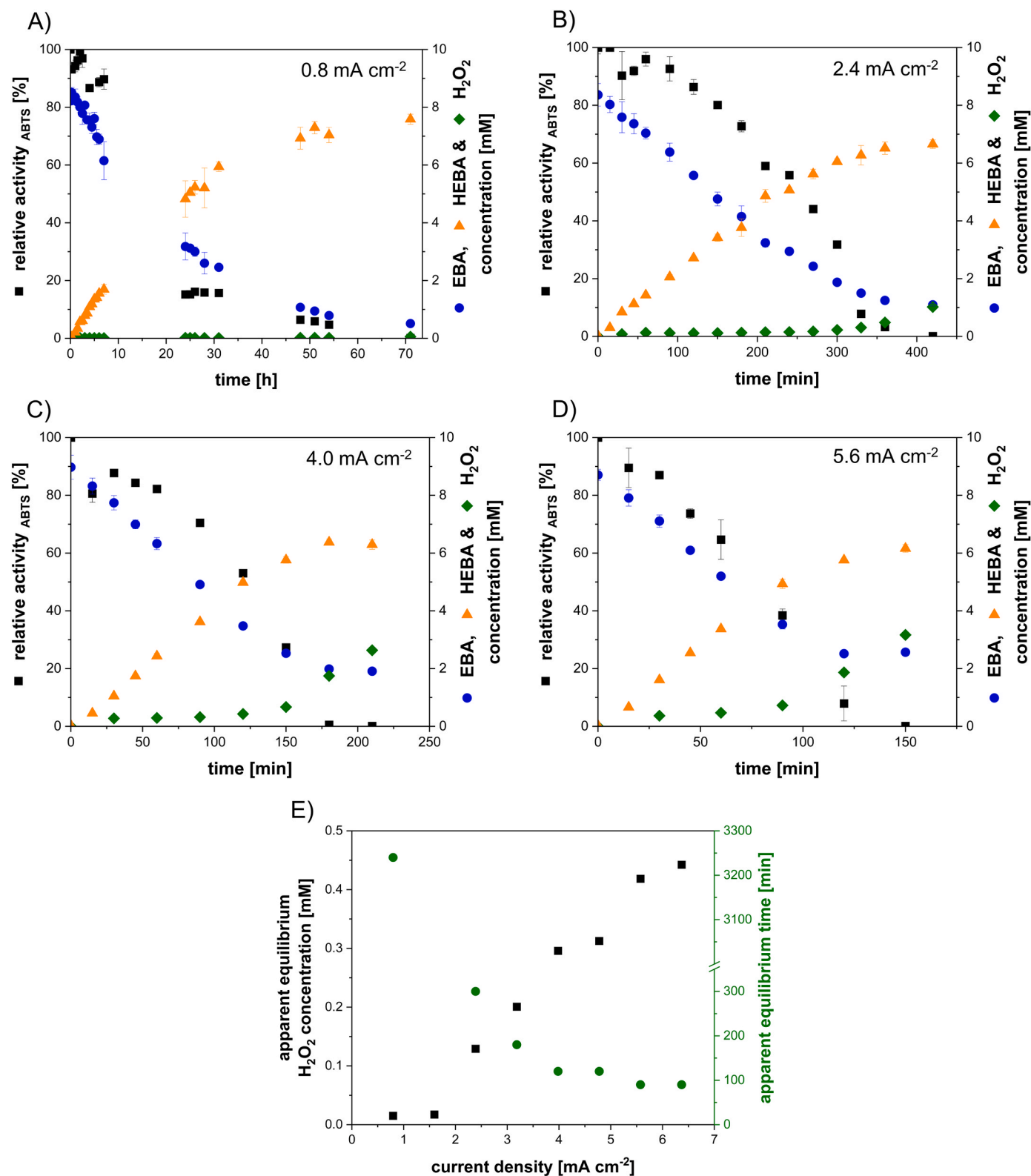


Fig. 3. Hydroxylation of EBA catalyzed by rAaeUPO in a GDE system with *in-situ* H₂O₂ generation at A) 0.8 mA cm⁻², B) at 2.4 mA cm⁻², C) at 4.0 mA cm⁻² and D) at 5.6 mA cm⁻². Reaction conditions: 200 mL 0.1 M KP₁ pH 7, 8 mM EBA, 10 nM rAaeUPO, 250 rpm, temperature: 22 ± 1 °C. EBA: 4-ethylbenzoic acid, HEBA: 4-(1-hydroxyethyl)benzoic acid. See Fig. S4. A-D for the full data set. E) Apparent equilibrium H₂O₂ concentration and apparent equilibrium time as a function of current density. The apparent equilibrium time describes the duration, in which the H₂O₂ concentration remains relatively constant during the experiment. The apparent equilibrium time is the duration until the H₂O₂ concentration deviates from the apparent equilibrium H₂O₂ concentration by 30%. The threshold of 30% was chosen due to overall low H₂O₂ concentrations during the experiment. Deviations below 30% were interpreted as minor fluctuations. Data shown are average from technical duplicates.

Nonetheless, the duration of linearity for the product formation differs for each current density. At lower applied current density such as 2.4 mA cm^{-2} , the formation rate stays within the linear range for a longer duration (210 min, Fig. 3B), whereas at higher current densities e.g., 5.6 mA cm^{-2} , the formation rate deviates from the linear range more quickly (90 min, Fig. 3D) due to higher substrate conversion rate and faster enzyme deactivation.

It is observable in Fig. 4 that the productivity and the TOF are increasing with increasing current density. The highest productivity and TOF obtained under the galvanostatic mode are $10.5 \text{ g L}^{-1} \text{ d}^{-1}$ and 76.7 s^{-1} , respectively. Both are achieved at the highest current density, 6.4 mA cm^{-2} . Meanwhile, the TTN reaches its maximum of approximately $650,000 \text{ mol mol}^{-1}$ at around 2.4 mA cm^{-2} and 3.2 mA cm^{-2} . An inverse behavior is observed as the current density is increased beyond 3.2 mA cm^{-2} . The TTN decreases to $500,000 \text{ mol mol}^{-1}$ at 6.4 mA cm^{-2} . The increasing productivity and TOF could not compensate the faster enzyme deactivation as the current density was increased above 3.2 mA cm^{-2} . A faster enzyme deactivation resulted in a reduced final product concentration before all enzyme was deactivated, leading to a decrease in the TTN. A fluctuation in TOF is observed, decreases from 66 s^{-1} to 55 s^{-1} at 4.8 mA cm^{-2} and increases again to 73 s^{-1} at 5.6 mA cm^{-2} . This observed trend could potentially represent an isolated deviation. Furthermore, other literatures have reported a trend of TOF either remaining stagnant or decreasing with increasing current density, without exhibiting fluctuations [21,26]. The maximum TTN obtained under the galvanostatic mode is higher compared to those reported in literatures ($400,000 \text{ mol mol}^{-1}$) using a GDE-based system [19,21]. A higher TTN obtained here can be explained by a higher enzyme stability due to comparably lower H_2O_2 productivity. The maximum H_2O_2 productivity achieved in this study is between 5.8 and 41 times lower [19,21]. The relatively small ratio of 0.12 between the counter electrode and the working electrode surface area may restrict the electron flow, potentially diminishing the overall efficiency of the working electrode. This could be an explanation for the observed low H_2O_2 productivity, especially when considering that other literatures have reported ratios of 0.8 and 1, which could lead to improved performance [19,21]. Due to lower H_2O_2 productivity, the obtained TOF and the productivity are 1.7 and 2.4 times lower, respectively [19,21].

Electroenzymatic hydroxylation of EBA under H_2O_2 -stat mode

The results from the electroenzymatic hydroxylation of EBA conducted under the galvanostatic mode, discussed in the previous section, served as a reference in this study. Herein, electroenzymatic

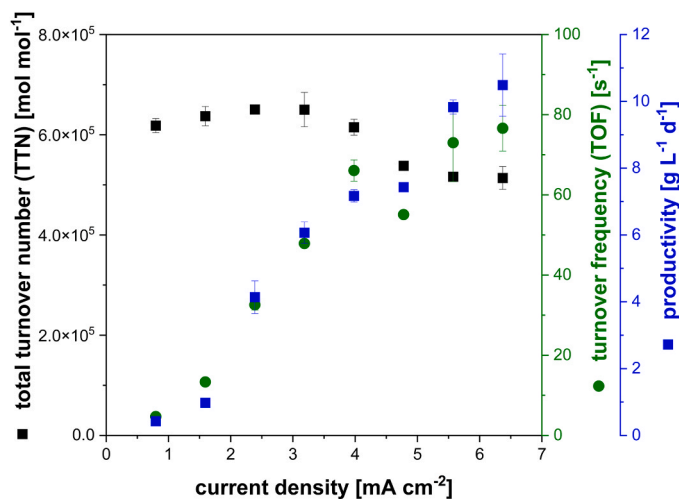


Fig. 4. Corresponding TTN, TOF and productivity as a function of current density. Data shown are average from technical duplicates.

experiments were conducted once again, this time utilizing the H_2O_2 -stat mode at a concentration limit set between 0.06 mM and 0.28 mM, with the intention to increase the enzyme stability and the TTN.

In the H_2O_2 -stat mode, the H_2O_2 concentration increases to a pre-determined concentration and a steady concentration is maintained throughout the experiment. This is automated via LabVIEW by regulating the electrical current output of the power supply, therefore delivering a dynamic current to the electrodes based on the input from the H_2O_2 sensor, which measures the H_2O_2 concentration in the medium. Fig. 5A-D illustrate the results from the hydroxylation of EBA performed under the H_2O_2 -stat mode with the H_2O_2 concentration limit set to 0.06 mM, 0.15 mM, 0.2 mM and 0.28 mM, respectively. As soon as the experiment is initiated by engaging the automation system, the power supply increases the current output towards the electrodes to increase the H_2O_2 productivity and to reach its respective H_2O_2 concentration limit.

Moreover, in Fig. 6A, the resulting current density, measured H_2O_2 concentrations, and enzyme relative activity over time obtained from the experiment performed under the H_2O_2 -stat mode with the H_2O_2 limit set to 0.15 mM are plotted together. This assessment is performed for the set concentration of 0.15 mM solely for the purpose of exemplifying the automation system and thus, the changes in the current density throughout the experiment, allowing for adjustments of H_2O_2 productivity. It is apparent from Fig. 6A that the current density is increased to 4 mA cm^{-2} within the first 15 min and remains relatively constant up to 60 min. Correspondingly, the H_2O_2 concentration increases to its limit of 0.15 mM. The measured H_2O_2 concentration is stable for the whole duration of the experiment. Parallel to the online quantification using the H_2O_2 sensor, the H_2O_2 concentrations were also quantified using an offline photometrical method (indicated as H_2O_2 offline) as a validation of the H_2O_2 sensor values. In this regard, a maximum deviation of 0.03 mM was observed between the offline and online H_2O_2 quantification. The observed deviation could be attributed to the use of different calibration systems for each method. The online quantification method, utilizing the H_2O_2 sensor, employs an internal 2-points calibration (set by the manufacturer) with calibration points set at 0 mM and 0.294 mM, which correspond to the theoretical zero value and upper detection limit, respectively. On the other hand, the offline quantification method utilizes a 9-points calibration, with calibration points ranging from 0 mM to 0.1 mM (Suppl. Fig. S3). The observed deviation during the experiment was likely due to reaching the practical lower quantification limit of the online method. This is due to the utilization of a 2-points calibration, which provides fewer reference points. Especially, at lower concentration ranges, resulting in less precise detection of H_2O_2 . This is reflected in the fact that the highest deviation between the offline and online H_2O_2 quantification was found in the experiment performed at the H_2O_2 -stat concentration of 0.06 mM (Fig. 5A). This highlights the importance of performing an offline quantification as a control to an online quantification. After 60 min (Fig. 6A), the current density is steadily decreasing and starts to mimic the declining trend of the relative enzyme activity and the substrate concentration (Fig. 5B). The current output and thus, the current density is reduced to lower the H_2O_2 productivity since the enzymatic H_2O_2 consumption is also declining as the enzyme activity decreases. In this way, the amount of generated H_2O_2 is adjusted to stay equal to the amount of consumed H_2O_2 keeping the H_2O_2 concentration constant in the reaction medium.

In general, the final product concentration obtained and the duration of the reaction decrease when the H_2O_2 -stat concentration limit is increased. By raising the H_2O_2 concentration limit, the availability of the co-substrate increases, leading to a higher reaction rate ($K_M, \text{H}_2\text{O}_2$: 1.3–1.8 mM [5,21,32]). Correspondingly, both TOF and the productivity increase, reaching a maximum of 87.5 s^{-1} and $6.9 \text{ g L}^{-1} \text{ d}^{-1}$, respectively (Fig. 6B). Additionally, reaching a high TOF and reaction rate at a higher H_2O_2 -stat concentration limit also increases the possibility of rAaeUPO undergoing catalase and catalase malfunction

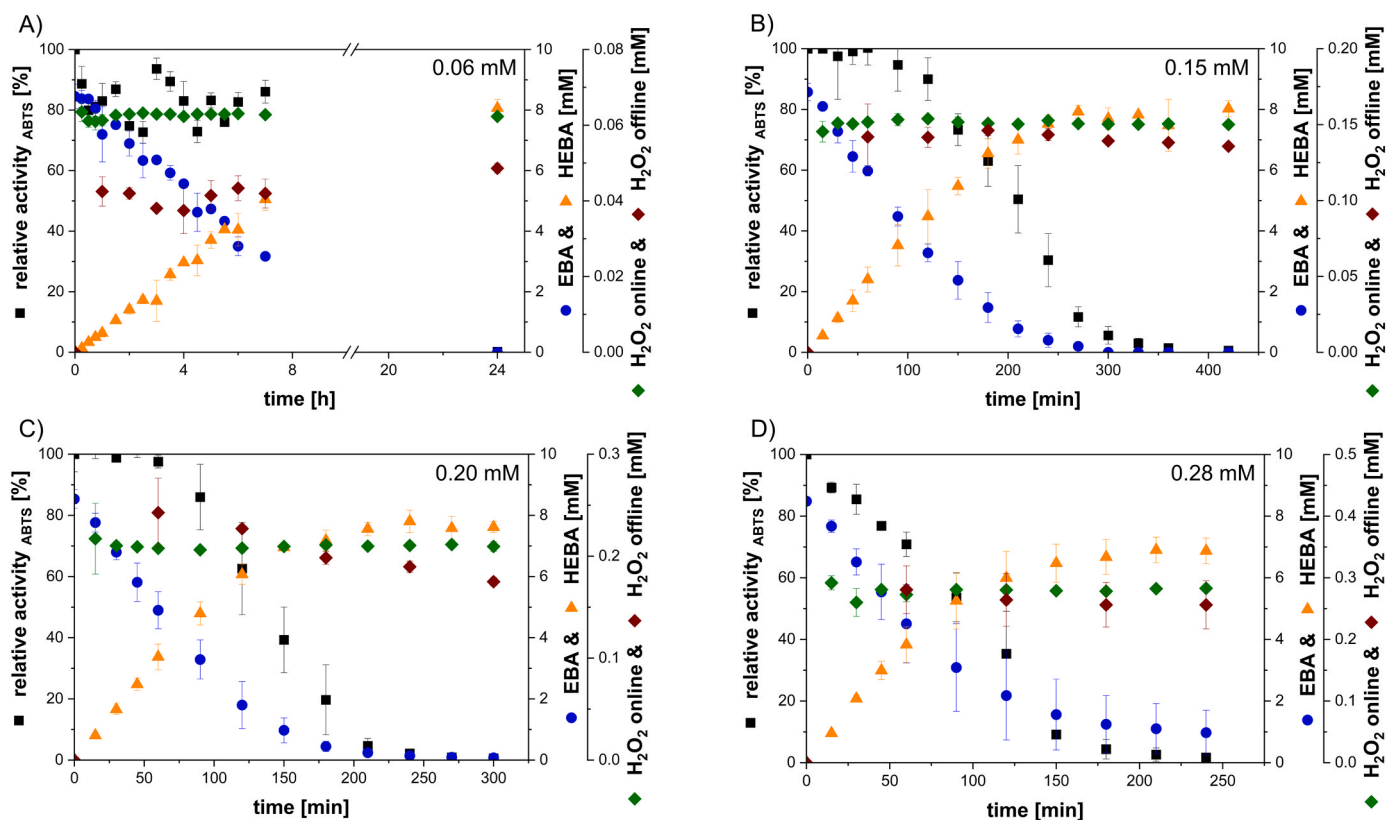


Fig. 5. Hydroxylation of EBA catalyzed by rAaeUPO in a GDE system operating in H₂O₂-stat mode with the H₂O₂ limit set to A) 0.06 mM, B) 0.15 mM, C) 0.2 mM and D) 0.28 mM. Reaction conditions: 200 mL 0.1 M KP_i pH 7, 8 mM EBA, 10 nM rAaeUPO, 250 rpm, temperature: 22 ± 1 °C. EBA: 4-ethylbenzoic acid, HEBA: 4-(1-hydroxyethyl)benzoic acid. H₂O₂ offline: an offline H₂O₂ quantification via a photometrical method serves as a control for the online quantification. Duplicates were performed.

reactions [8,21]. The reason for the aforementioned reactions is that the highly reactive species of rAaeUPO (termed as compound I) formed after binding with the first H₂O₂ molecule, can react not only with the substrate EBA to yield the product HEBA, but also with a second and third H₂O₂ molecule [8,21]. The reaction of compound I with the second H₂O₂ molecule yields compound II. Compound II can further react with H₂O₂, yielding compound III. The formation of compound III would eventually lead to a heme-bleaching and irreversible enzyme deactivation [8,21]. Moreover, the catalase and catalase malfunction reactions become more pronounced at lower substrate concentrations [15]. For EBA, a K_M of 2.3 mM was reported [21]. In this case, reaching EBA concentrations below its K_M leads not only to a reduced reaction rate but also prompting the catalase malfunction reaction due to constant availability of H₂O₂ in the medium, leading to a faster enzyme deactivation with increasing H₂O₂-stat concentration limit (Fig. 6C). This also decreases the obtained final product concentration. The final sampling point for the experiment conducted at the H₂O₂-stat limit of 0.06 mM (Fig. 5A) was taken after 24 h. By this time, the enzyme had already been deactivated. Therefore, the enzyme operational lifetime was determined based on the point where the current density was reduced and stabilized (by the automation system) at around 0.16 mA cm⁻². At this current density, the H₂O₂ productivity had ceased, effectively preventing its accumulation, due to the absence of H₂O₂ consumption by the enzyme. Regarding the product HEBA, no product inhibition was observed, at least up to 8 mM.

Overall, the highest analytical yield achieved in this study was 95%. The TTN decreases from the maximum of 710,000 mol mol⁻¹ at a H₂O₂-stat setting of 0.15 mM to 570,000 mol mol⁻¹ at 0.28 mM (Fig. 6B). Although the highest TTN is obtained at a set concentration of 0.15 mM, the corresponding TOF (58.0 s⁻¹) and productivity (4.6 g L⁻¹ d⁻¹) are far from the maximum. As the H₂O₂ concentration limit is increased

from 0.15 mM to 0.2 mM, the TOF increases to 80.3 s⁻¹ and the productivity increases to 6.1 g L⁻¹ d⁻¹. Nevertheless, further increasing the H₂O₂-stat concentration from 0.2 mM to 0.28 mM does not significantly increase the TOF and productivity anymore. Therefore, under these circumstances and in this specific system, it is recommended to set the H₂O₂-stat concentration to 0.2 mM as this concentration limit allows not only the achievement of comparably high TOF and productivity, but also a competitive TTN (655,000 mol mol⁻¹), compared to other reported TTNs from comparable reaction systems in a lab-scale (Table 1).

Comparing the key performance indicators from the electro-enzymatic experiments conducted under the galvanostatic mode and under H₂O₂-stat operation, the maximum TOF achieved using both methods are comparable (Fig. 4, Fig. 6B). However, the highest productivity achieved under the galvanostatic method (10.5 g L⁻¹ d⁻¹) is higher compared to the one obtained under the H₂O₂-stat mode (6.9 g L⁻¹ d⁻¹). A higher productivity under the galvanostatic method can be explained by a higher H₂O₂ productivity and a higher accumulation of H₂O₂ in the medium. However, due to a higher and an ever-increasing accumulation of H₂O₂ under the galvanostatic method, leading to a faster enzyme deactivation, the obtained final product concentration and the TTN decrease. In this regard, the maximum TTN acquired under the H₂O₂-stat mode is 10% higher compared to the maximum TTN acquired under the galvanostatic method. Under an optimum condition (H₂O₂-stat mode: 0.2 mM, galvanostatic mode: 3.2 mA cm⁻²), the experiment conducted under H₂O₂-stat mode still has a higher TTN (655,000 mol mol⁻¹) and TOF (80.3 s⁻¹), as well as a similar productivity (6.1 g L⁻¹ d⁻¹). In Table 1, the impact of various H₂O₂ supply methods on the enzyme stability and thus, also on the TTN for H₂O₂-dependent enzymatic reactions are listed. The TTN serves as an important metric to assess the suitability of a biocatalyst for a specific process. It also effectively correlates the yield of the product to the input

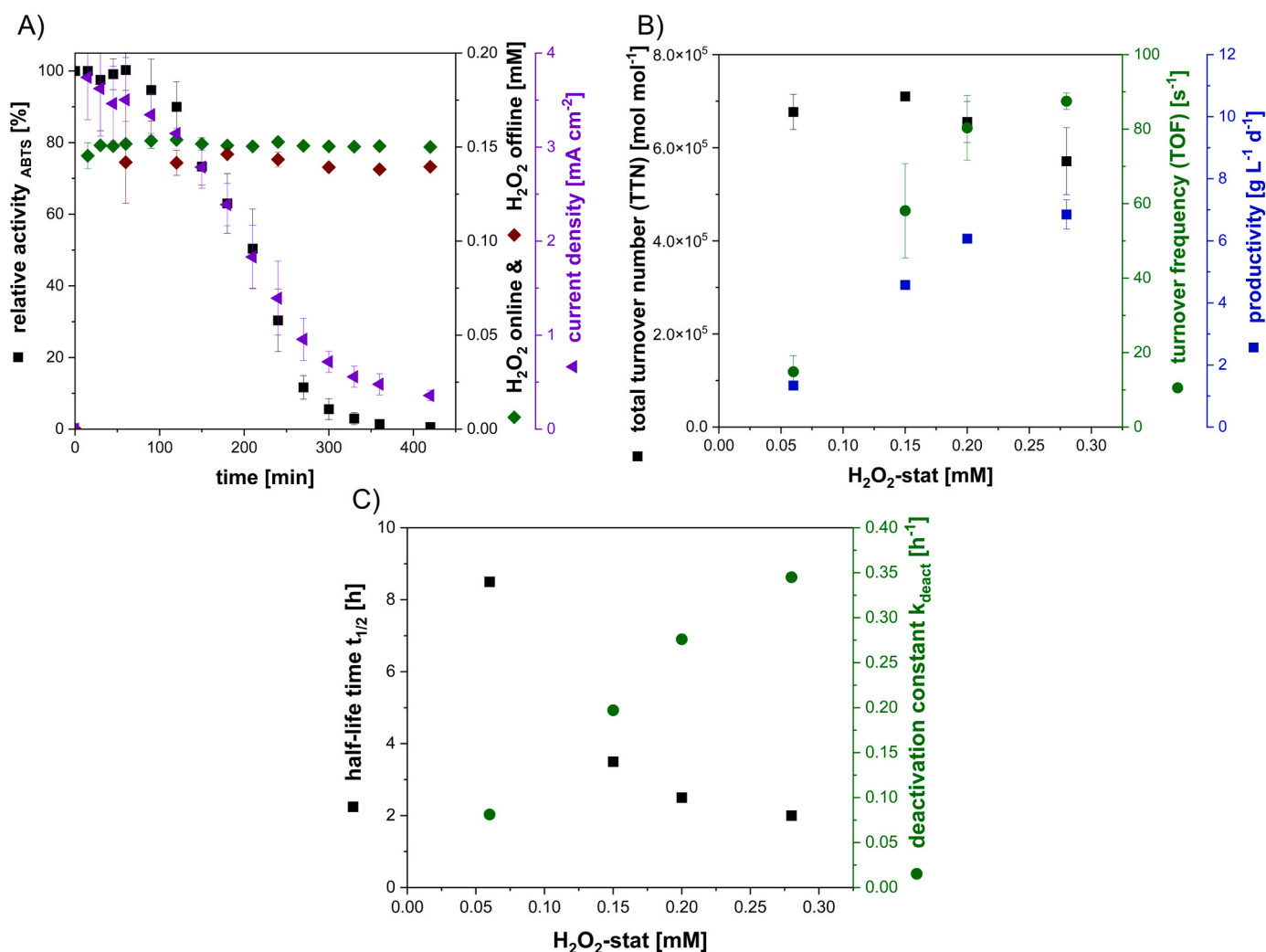


Fig. 6. A) Time-dependent relative enzyme activity, current density and H_2O_2 concentrations for the hydroxylation of EBA operated under H_2O_2 -stat mode with the H_2O_2 limit set to 0.15 mM. H_2O_2 offline: an offline H_2O_2 quantification via a photometrical method serves as a control for the online quantification. B) Corresponding TTN, TOF and productivity as a function of the set H_2O_2 -stat concentration. C) Half-life time ($t_{1/2}$) and deactivation constant (k_{deact}) of rAaeUPO at different H_2O_2 -stat concentrations. The half-life time of rAaeUPO was determined by dividing the actual enzyme operational lifetime observed during the experiment (experiments shown in Fig. 5. A-D) by two. Deactivation constant was determined from the half-life time ($t_{1/2}$). $k_{deact} = \frac{\ln(2)}{t_{1/2}}$. Duplicates were performed.

Table 1

Comparison of the impact of different H_2O_2 supply method on the total turnover number (TTN) of H_2O_2 -dependent enzymatic reactions.

Substrate, enzyme	Reaction system	TTN [$mol\ mol^{-1}$]	Literature
Indole, CPO	Batch, sensor-controlled feeding of H_2O_2	644,000	[9]
Thioanisole, CPO	Batch, <i>in-situ</i> electrogeneration of H_2O_2 (galvanostatic)	145,000	[15]
Ethylbenzene, rAaeUPO	Batch, immobilized enzyme, manual feeding of H_2O_2	900,000	[33]
Ethylbenzene, rAaeUPO	Batch, enzymatic <i>in-situ</i> generation of H_2O_2	470,000	[34]
Ethylbenzene, rAaeUPO	Batch, GDE-based system (galvanostatic)	400,000	[19]
EBA, rAaeUPO	Batch, GDE-based system, H_2O_2 -stat mode (0.5 mM)	360,000	[21]
EBA, rAaeUPO	Batch, GDE-based system, H_2O_2 -stat mode (0.15 mM)	710,000	This study

of the catalyst, providing valuable insights in cost valuation of a reaction system. The highest TTN ($900,000\ mol\ mol^{-1}$) for rAaeUPO-catalyzed hydroxylation reaction was found in a batch system with manual feeding of H_2O_2 and immobilized enzyme [33]. Compared to the highest TTN reported in literature, the highest TTN in this study is around 20% lower. However, the electrogeneration of H_2O_2 eliminates the need for a second enzyme or volume increase. Additionally, the GDE system offers key advantages, including easy technical set-up and elimination of O_2 mass transfer limitations. The higher TTN reported in the literature previously can be attributed to enhanced enzyme operational stability resulting from the enzyme immobilization. Enzyme immobilization has been recognized as a significant approach to enhance the performance of bioelectrochemical systems, as also indicated in other literature [20,27]. This aspect could serve as an optimization point for the system presented in this study. Furthermore, while the current productivity is low, there is potential for future commercial applications with optimization. An optimization of the productivity under the H_2O_2 -stat mode could potentially be achieved by employing a fed-batch or continuous process

in order to ensure a constant substrate concentration above the K_M value and the application of immobilization technique to increase the enzyme stability.

Conclusion

It is clear that the mode of H_2O_2 electrogeneration impacts the enzyme's operational stability and the overall productivity. The presented results demonstrate that each mode has its own advantages and disadvantages. On the one hand, galvanostatic mode offers a higher productivity at a higher current density but suffers from a faster enzyme deactivation due to a continuously increasing concentration of H_2O_2 and, therefore, excess of H_2O_2 . As a result, the final product concentration and the TTN are reduced. On the other hand, operation under H_2O_2 -stat condition provides the possibility to achieve high TOF and TTN, albeit at a lower productivity. The advantage of the H_2O_2 -stat mode lies in its ability to adapt to the changes of the H_2O_2 consumption rate over time, in accordance to the progress of the reaction. Therefore, an excess of H_2O_2 is prevented protecting the enzyme from rapid deactivation. The key performance indicators such as productivity and TOF obtained under the H_2O_2 -stat mode are comparable to those reported in literature. Notably, the TTN obtained in this study is higher than all reported values for rAaeUPO-catalyzed reaction in bio-electrochemical systems, to the best of our knowledge. Furthermore, in order to gain a comprehensive understanding of the inactivation mechanism in different H_2O_2 -dependent enzymes, the H_2O_2 -stat method introduced here can be applied in the study of these enzymes.

Declaration of Generative AI and AI-assisted technologies in the writing process

During the preparation of this work the author(s) used ChatGPT in order to improve the readability. After using this tool, the author(s) reviewed and edited the content as needed and take(s) full responsibility for the content of the publication.

Declaration of Competing Interest

The authors declare that they have no known competing financial interests or personal relationships that could have appeared to influence the work reported in this paper.

Data availability

Data will be made available on request.

Acknowledgements

This work was supported by the Deutsche Forschungsgemeinschaft (DFG, German Research Foundation, e-Biotech SPP 2240) (Project number: 445947004). Publishing fees supported by Funding Program Open Access Publishing of Hamburg University of Technology (TUHH). The authors thank Fernando Lopez Haro from the TUHH for the preparation of the graphical abstract.

Appendix A. Supporting information

Supplementary data associated with this article can be found in the online version at [doi:10.1016/j.nbt.2023.10.007](https://doi.org/10.1016/j.nbt.2023.10.007).

References

- [1] Ullrich R, Nüske J, Scheibner K, Spantzel J, Hofrichter M. Novel haloperoxidase from the agaric basidiomycete *Agrocybe aegerita* oxidizes aryl alcohols and aldehydes. *Appl Environ Microbiol* 2004;70:4575–81.
- [2] Hofrichter M, Ullrich R. Oxidations catalyzed by fungal peroxigenases. *Curr Opin Chem Biol* 2014;19:116–25. <https://doi.org/10.1016/j.cbpa.2014.01.015>.
- [3] Hofrichter M, Kellner H, Pecyna MJ, Ullrich R. Fungal Unspecific Peroxygenases: Heme-thiolate proteins that combine peroxidase and cytochrome P450 Properties. In: Hrycay EG, Bandiera SM, editors. *Monooxygenase Peroxidase Peroxygenase Prop. Mech. Cytochrome P450*, vol. 851. Cham: Springer International Publishing; 2015. p. 341–68. https://doi.org/10.1007/978-3-319-16009-2_13.
- [4] Godula K, Sames D. C-H bond functionalization in complex organic synthesis. *Science* 2006;312:67–72. <https://doi.org/10.1126/science.1114731>.
- [5] Molina-Espeja P, Ma S, Mate DM, Ludwig R, Alcalde M. Tandem-yeast expression system for engineering and producing unspecific peroxigenase. *Enzym Micro Technol* 2015;73–74:29–33. <https://doi.org/10.1016/j.enzmictec.2015.03.004>.
- [6] Brummund J, Müller M, Schmitges T, Kaluzna I, Mink D, Hilterhaus L, et al. Process development for oxidations of hydrophobic compounds applying cytochrome P450 monooxygenases *in-vitro*. *J Biotechnol* 2016;233:143–50. <https://doi.org/10.1016/j.jbiotec.2016.07.002>.
- [7] Bernhardt R. Cytochromes P450 as versatile biocatalysts. *J Biotechnol* 2006;124:128–45. <https://doi.org/10.1016/j.jbiotec.2006.01.026>.
- [8] Karich A, Scheibner K, Ullrich R, Hofrichter M. Exploring the catalase activity of unspecific peroxigenases and the mechanism of peroxide-dependent heme destruction. *J Mol Catal B Enzym* 2016;134:238–46. <https://doi.org/10.1016/j.molcatb.2016.10.014>.
- [9] Seelbach K, van Deurzen MPJ, van Rantwijk F, Sheldon RA, Kragl U. Improvement of the total turnover number and space-time yield for chloroperoxidase catalyzed oxidation. *Biotechnol Bioeng* 1997;55:283–8. [https://doi.org/10.1002/\(SICI\)1097-0290\(19970720\)55:2<283::AID-BIT6>3.0.CO;2-E](https://doi.org/10.1002/(SICI)1097-0290(19970720)55:2<283::AID-BIT6>3.0.CO;2-E).
- [10] Lütz S, Steckhan E, Liese A. First asymmetric electroenzymatic oxidation catalyzed by a peroxidase. *Electrochem Commun* 2004;6:583–7. <https://doi.org/10.1016/j.elecom.2004.04.009>.
- [11] van de Velde F, van Rantwijk F, Sheldon RA. Selective oxidations with molecular oxygen, catalyzed by chloroperoxidase in the presence of a reductant. *J Mol Catal B Enzym* 1999;6:453–61. [https://doi.org/10.1016/S1381-1169\(99\)00059-X](https://doi.org/10.1016/S1381-1169(99)00059-X).
- [12] van de Velde F, Lourenço ND, Bakker M, van Rantwijk F, Sheldon RA. Improved operational stability of peroxidases by coimmobilization with glucose oxidase. *Biotechnol Bioeng* 2000;69:286–91. [https://doi.org/10.1002/1097-0290\(20000805\)69:3<286::AID-BIT6>3.0.CO;2-R](https://doi.org/10.1002/1097-0290(20000805)69:3<286::AID-BIT6>3.0.CO;2-R).
- [13] Yoon J, Kim J, Tieves F, Zhang W, Alcalde M, Hollmann F, et al. Piezobiocatalysis: ultrasound-driven enzymatic oxyfunctionalization of C–H bonds. *ACS Catal* 2020;10:5236–42. <https://doi.org/10.1021/acscatal.0c00188>.
- [14] Burek BO, de Boer SR, Tieves F, Zhang W, van Schie M, Bormann S, et al. Photoenzymatic hydroxylation of ethylbenzene catalyzed by unspecific peroxigenase: origin of enzyme inactivation and the impact of light intensity and temperature. *ChemCatChem* 2019;11:3093–100. <https://doi.org/10.1002/cctc.201900610>.
- [15] Lütz S, Vuorilehto K, Liese A. Process development for the electroenzymatic synthesis of (R)-methylphenylsulfonide by use of a 3-dimensional electrode. *Biotechnol Bioeng* 2007;98:525–34. <https://doi.org/10.1002/bit.21434>.
- [16] Stöckl M, Lange T, Izadi P, Bolat S, Teetz N, Harnisch F, et al. Application of gas diffusion electrodes in bioeconomy—an update. *Biotechnol Bioeng* 2023.
- [17] Horst AEW, Mangold K-M, Holtmann D. Application of gas diffusion electrodes in bioelectrochemical syntheses and energy conversion. *Biotechnol Bioeng* 2016;113:260–7. <https://doi.org/10.1002/bit.25698>.
- [18] Bormann S, van Schie MM, De Almeida TP, Zhang W, Stöckl M, Ulber R, et al. H_2O_2 production at low overpotentials for electroenzymatic halogenation reactions. *ChemSusChem* 2019;12:4759–63.
- [19] Horst AEW, Bormann S, Meyer J, Steinhagen M, Ludwig R, Drews A, et al. Electroenzymatic hydroxylation of ethylbenzene by the evolved unspecific peroxigenase of *Agrocybe aegerita*. *J Mol Catal B Enzym* 2016;133:S137–42. <https://doi.org/10.1016/j.molcatb.2016.12.008>.
- [20] Holtmann D, Krieg T, Getrey L, Schrader J. Electroenzymatic process to overcome enzyme instabilities. *Catal Commun* 2014;51:82–5.
- [21] Bormann S, Hertweck D, Schneider S, Bloh JZ, Ulber R, Spiess AC, et al. Modeling and simulation-based design of electroenzymatic batch processes catalyzed by unspecific peroxigenase from *A. aegerita*. *Biotechnol Bioeng* 2021;118:7–16.
- [22] Invitrogen. *Pichia Fermentation Process Guidelines* 2002.
- [23] Cino J. High-yield protein production from *Pichia pastoris* yeast: A protocol for benchtop fermentation. *Am Biotechnol Lab* 1999;17:10–3.
- [24] Perz F, Bormann S, Ulber R, Alcalde M, Bubenheim P, Hollmann F, et al. Enzymatic oxidation of butane to 2-butanol in a bubble column. *ChemCatChem* 2020;12:3666–9.
- [25] Khataee AR, Safarpour M, Zarei M, Aber S. Electrochemical generation of H_2O_2 using immobilized carbon nanotubes on graphite electrode fed with air: investigation of operational parameters. *J Electro Chem* 2011;659:63–8. <https://doi.org/10.1016/j.jelechem.2011.05.002>.
- [26] Sayoga GV, Bueschler VS, Beisch H, Holtmann D, Zeng A-P, Fiedler B, et al. Application of the all-in-one electrode for *in situ* H_2O_2 generation in hydroxylation

- catalyzed by unspecific peroxygenase from *Agroclybe aegerita*. *Mol Catal* 2023;547: 113325. <https://doi.org/10.1016/j.mcat.2023.113325>.
- [27] Krieg T, Hüttmann S, Mangold K-M, Schrader J, Holtmann D. Gas diffusion electrode as novel reaction system for an electro-enzymatic process with chloroperoxidase. *Green Chem* 2011;13:2686–9. <https://doi.org/10.1039/C1GC15391A>.
- [28] Peralta E, Natividad R, Roa G, Marin R, Romero R, Pavon T. A comparative study on the electrochemical production of H₂O₂ between BDD and graphite cathodes. *Sustain Environ Res* 2013;23:259–66.
- [29] Wang Y, Liu Y, Wang K, Song S, Tsiakaras P, Liu H. Preparation and characterization of a novel KOH activated graphite felt cathode for the electro-Fenton process. *Appl Catal B Environ* 2015;165:360–8. <https://doi.org/10.1016/j.apcatb.2014.09.074>.
- [30] Panizza M, Cerisola G. Electrochemical generation of H₂O₂ in low ionic strength media on gas diffusion cathode fed with air. *Electrochim Acta* 2008;54:876–8.
- [31] Kim G-Y, Lee K-B, Cho S-H, Shim J, Moon S-H. Electroenzymatic degradation of azo dye using an immobilized peroxidase enzyme. *J Hazard Mater* 2005;126:183–8.
- [32] Kluge MG, Ullrich R, Scheibner K, Hofrichter M. Spectrophotometric assay for detection of aromatic hydroxylation catalyzed by fungal haloperoxidase–peroxygenase. *Appl Microbiol Biotechnol* 2007;75:1473–8.
- [33] Hobisch M, De Santis P, Serban S, Basso A, Byström E, Kara S. Peroxygenase-driven ethylbenzene hydroxylation in a rotating bed reactor. *Org Process Res Dev* 2022; 26:2761–5.
- [34] Ni Y, Fernández-Fueyo E, Baraibar AG, Ullrich R, Hofrichter M, Yanase H, et al. Peroxygenase-catalyzed oxyfunctionalization reactions promoted by the complete oxidation of methanol. *Angew Chem Int Ed* 2016;55:798–801. <https://doi.org/10.1002/anie.201507881>.